IS-PORTO 2023 PROCEEDINGS

Proceedings of the 8th International Symposium on DEFORMATION CHARACTERISTICS OF GEOMATERIALS Porto, 3rd - 6th September 2023

In-situ material damping measurements using the crosshole seismic method

Sungmoon Hwang[1], and *Kenneth* H. Stokoe, II[2#]

[1]*University of Texas at Austin, Civil, Architectural and Environmental Engineering, Austin, USA*
[2] *University of Texas at Austin, Civil, Architectural and Environmental Engineering, Austin, USA*
[#]*Corresponding author: k.stokoe@mail.utexas.edu*

ABSTRACT

Crosshole seismic testing is commonly used to determine detailed and reliable wave velocity profiles. Material damping measurements can also be performed in crosshole seismic testing, but these measurements require a window function to maintain similar amplitude shapes over the frequency range of interest for the calculation. In-situ seismic testing, including downhole and seismic cone penetration testing (SCPT), also requires a window function for the material damping calculations. However, the length of the window function has the largest influence on the material damping calculation. Therefore, the half-power bandwidth method is introduced to determine the material damping ratio without the window function in crosshole testing by replicating the unconfined, free-free, resonant column (Fr-Fr) test. To demonstrate the influence in the length of the window function, the first cycle of the signal is used in the material damping calculation. The half- power bandwidth method is verified using synthetic signals and field data. Two sets of crosshole and downhole tests were performed, one at a backfill test pad and the second at a Hornsby Bend research site operated by the University of Texas at Austin. The in-situ material damping ratio calculated from these two sets of crosshole tests using the half-power bandwidth method are compare with the Spectral Ratio Slope (SRS) method applied to the downhole testing at these sites. The material damping calculated from the half-power bandwidth method using the full signal results in a reliable and precise damping value compared to the SRS method applied to the downhole data.

Keywords: Crosshole seismic testing; in-situ material damping ratio; half-power bandwidth method; window function.

1. Introduction

In-situ seismic testing methods are generally used in geotechnical engineering to determine the wave velocity profiles of body waves, constrained compression (P) and shear (S) waves. Since body wave velocities are directly linked to elastic moduli of the geotechnical material, various in-situ seismic testing methods have been developed.

On the other hand, material damping ratio is traditionally determined from laboratory tests since accurate measurements over a range in strain levels can be performed using the half-power bandwidth and free-vibration decay methods. Despite the fact that accurate material damping measurements can be performed in the laboratory, there are also disadvantages emphasizing the need for and importance of the in-situ damping measurements. First, laboratory testing can only approximate the field conditions. The 3-D in-situ stress state, the in-situ soil structure, and in-situ inhomogeneity are not replicated in the laboratory. Second, disturbances during sampling of the soil, especially in granular soils, are avoided by the in-situ testing.

To overcome the disadvantages of laboratory testing and produce more direct material damping measurements, various approaches have been developed mainly using crosshole (Mok et al. 1988), downhole (Tonouci et al. 1983), and SCPT (Stewart and Campanella 1991, 1993) in-situ testing methods.

Mok et al. 1998 and Tonouci et al. 1983 used the coefficient of attenuation, α, to calculate material damping ratio. The coefficient of attenuation in the crosshole testing method is determined by the ratio of the amplitude and distance between two signals as shown in the following equation (Mok et al. 1988):

$$\alpha(f_n) = \frac{\ln\left(\frac{X_1(f_n)\cdot r_1}{X_2(f_n)\cdot r_2}\right)}{\Delta r} \quad (1)$$

where $X_1(f_n)$ and $X_2(f_n)$ are amplitude of the FFT of two signals at receiver locations r_1 and r_2, respectively.

The coefficient of attenuation in the downhole testing method is determined by the ratio of the normalized amplitude and distance between two signals as shown in the following equation (Tonouci et al. 1983):

$$\alpha(f_n) = \frac{\ln\left(\frac{X_1(f_n)/Y_1(f_n)\cdot r_1}{X_2(f_n)/Y_2(f_n)\cdot r_2}\right)}{\Delta r} \quad (2)$$

where $Y_1(f_n)$ and $Y_2(f_n)$ are the amplitudes of the FFTs of two signals at a shallow reference receiver location and $X_1(f_n)$ and $X_2(f_n)$ are the amplitude of the FFT of two signals at deeper receiver locations r_1 and r_2, respectively. The attenuation coefficient can also be represented by material damping ratio, D, with assumptions that the material damping ratio is independent of frequency and strain amplitude as shown in the following equation:

$$\alpha = \frac{2\pi f\cdot D}{V} \quad (3)$$

where f is frequency, D is the material damping ratio and V is the wave velocity. The material damping ratio can be determined using the relationship between Eqs. (1) and (3) or Eqs. (2) and (3).

Stewart and Campanella proposed the spectral ratio slope (SRS) method which uses the slope of the logarithmic ratio for the material damping calculation as shown in the following two equations:

$$k = \frac{\partial^2\left(-\ln\frac{X_r}{X_0}\right)}{\partial f \partial r} \quad (4)$$

$$D = \frac{k \cdot V}{2\pi} \quad (5)$$

where r is the distance, X_0 is the amplitude of the FFT of the signal at the reference receiver location, X_r is the amplitude of the FFT of the signal at a deeper receiver location, V is the wave velocity and D is the material damping ratio. Eq. (5) removes the geometrical corrections from the damping calculation which leads to the most reliable and consistent approach. The SRS method gives promising results for large-depth interval distances in the same (hence, uniform) material. However, this method can only be applied to receivers located deeper than 3 to 5 m where the signal is not affected by the surface or a shallow surficial layer. In addition, selecting the frequency range for the linear slope can be subjective which can limit the precision and increase the variability in the material damping values.

In the application of any of these in-situ damping methods, all procedures recommend using a window function for reliable and consistent results. Generally, the first cycle of the signal is used, however, detailed criteria for selecting the length of the window function are generally not clearly explained. In addition, Karl et al. 2006 conclude that the length of the window function is the major factor influencing the material damping value and recommend avoiding the window function if it is possible.

In this paper, in-situ material damping measurements using the half-power bandwidth method by replicating the unconfined, free-free, resonant column (Fr-Fr) test are introduced to determine material damping ratio without the window function in crosshole testing. In this paper, a brief review of the Fr-Fr test is given and the way to replicate the Fr-Fr test using the signal from the in-situ crosshole testing is discussed. Then, the material damping calculation using the half- power bandwidth method is verified by synthetic signals generated using Eqs. (1) and (3). The waveform segmentation method is suggested for the guideline tool for the window function if needed. Two sets of crosshole and downhole tests were performed, one at a backfill test pad and the second at the Hornsby Bend research site for verification. The in-situ material damping calculated from these two sets of crosshole tests using the half-power bandwidth method is compared with Spectral Ratio Slope (SRS) method applied to the downhole testing.

2. Unconfined, free-free, resonant column test or Fr-Fr test

The Fr-Fr test is a simple and accurate test to evaluate material stiffnesses and material damping ratios of soil and rock specimens at small strains. The simplicity of the Fr-Fr set-up is shown in Fig. 1a which eliminates potential compliance problems such as equipment-induced damping in a torsional electrical motor and fixity of the bottom platen in a fixed-free, resonant column configuration (Stokoe et al. 1994).

In the Fr-Fr test, three body wave velocities can be evaluated. These wave velocities are: (1) unconstrained compression wave velocity (V_c), (2) constrained compression wave velocity (V_p), and (3) shear wave velocity (V_s). With the relationships between these velocities, three values of Poisson's ratios can also be evaluated. In the Fr-Fr test, measurements of the compressional and torsional resonant frequencies of the specimen are used to calculate the wave velocity using Eq. (6):

$$V = f_r \cdot \lambda = f_r \cdot 2 \cdot l \quad (6)$$

where f_r is the first-mode resonant frequency of the specimen as shown in Fig. 1b, λ is wavelength and l is the length of the specimen. The wavelength of the specimen in the free-free boundary condition is simply twice the length of the specimen. The material damping ratio of the specimen is calculated based on the width of the frequency response curve around the resonant frequency as shown in Fig. 1c. From the frequency

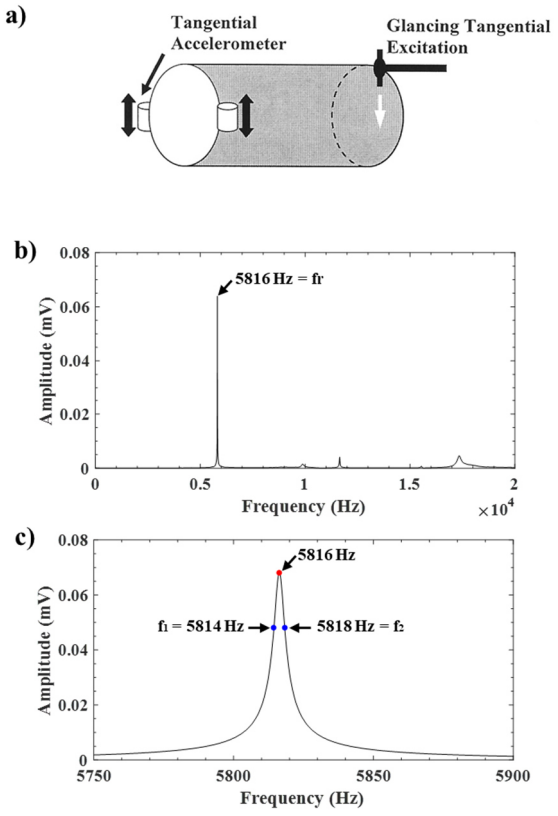

Figure 1. a) Fr-Fr test setup for torsional resonance testing, (b) power spectrum of the testing result with an aluminium specimen, and (c) expanded power spectrum of Fig 1.b around the resonant frequency, f_r

response curve, the logarithmic decrement can be calculated as shown in the following equation (Richart et al. 1970):

$$\delta = \frac{\pi}{2} \cdot \frac{f_2^2 - f_1^2}{f_r^2} \cdot \sqrt{\frac{A^2}{A_{max}^2 + A^2}} \cdot \frac{\sqrt{1-2D^2}}{1-2D^2} \quad (7)$$

where f_1 is the frequency below the resonant frequency where the amplitude is A, f_2 is the frequency above the resonance frequency where the amplitude is A, f_r is the resonant frequency, and D is the material damping ratio. If the material damping ratio is less than 0.1 (10%) and A is Amax$/\sqrt{2}$ which is called the half-power point, material damping ratio can be simplified as:

$$D = \frac{f_2 - f_1}{2f_r} \quad (8)$$

The Fr-Fr test was performed with an aluminum specimen as an example. These testing results are shown in Figs 1b and 1c. The length of the aluminum specimen was 26.65 cm. The torsional resonant frequency was 5816 Hz as shown in Fig. 1b. The shear wave velocity of the aluminum specimen was calculated using Eq. (6), and that was 3099 m/sec. The material damping ratio was calculated using Eq. (8) with f_1 was 5814 Hz and f_2 was 5818 Hz which resulted in D equal to 0.03%, a very low but reasonable value.

3. Half-power bandwidth method using the crosshole testing signal

To calculate the material damping ratio using the half-power bandwidth method, the resonant frequency of the structure needs to be determined. In the case of the Fr-Fr test, the resonant frequency is simply the one over the wave travel time from the one end to the other end and back where the tangential accelerometers were attached to measure the wave arrival as shown in Fig. 1a. The travel time can be easily calculated from the wave velocity. The shape of the frequency response curve as shown in Fig. 1b is determined by the frequency component and amplitude attenuation of the traveling wave until the wave dissipates after multiple arrivals. Therefore, if the velocity of the soil structure between the receiver locations can be determined and multiple waveforms can also be generated with constant amplitude attenuation using the crosshole testing signal, the material damping ratio can be calculated using the half-power bandwidth method.

The wave velocity can readily be determined from the crosshole signals between two receiver boreholes at the same depth either by picking a first arrival point on the time-domain waveforms or by applying the Spectral-Analysis-of-Body-Waves (SABW) method (Hwang 2018). The amplitude of the waveform at any distance representing the multiple arrivals of Fr-Fr testing can be generated using Eq. (1). Assuming the coefficient of attenuation is a constant between the crosshole receiver locations, the amplitude of the waveform at r_z can be given by Eq. (9)

$$\alpha(f_n) = \frac{\ln\left(\frac{X_1(f_n)\cdot r_1}{X_z(f_n)\cdot r_z}\right)}{(r_z - r_1)} \quad (9)$$

which gives:

$$X_z(f_n) = \frac{X_1(f_n)\cdot r_1}{e^{(\alpha(fn)\cdot(r_z - r_1))}\cdot r_z} \quad (10)$$

where $X_z(f_n)$ is the amplitude of the FFT of the signal at receiver location z. However, there is no geometrical amplitude attenuation term in the Fr-Fr test. As a result, the attenuation ratio in replicating the Fr-Fr test is defined by dividing Eq. (10) with geometrical amplitude attenuation as shown in Eq. (11):

$$\beta(f_n) = \frac{\frac{X_1(f_n)\cdot r_1}{e^{(\alpha(fn)\cdot(r_z - r_1))}\cdot r_z}}{\frac{X_1(f_n)\cdot r_1}{r_z}} = \frac{1}{e^{(\alpha(fn)\cdot(r_z - r_1))}} \quad (11)$$

4. Verification of the half-power bandwidth method using synthetic signals

Synthetic signals are created to verify the half-power bandwidth method for calculation of material damping ratio as illustrated in Fig 2. As shown in Fig. 2a, the black larger waveform represents the signal recorded at the near receiver location in crosshole testing. The signal was created by adding one cycle of sinusoidal waveforms from 305 to 500 Hz to have the frequency of the maximum amplitude of 300 Hz as shown in Fig. 2b. The blue waveform in Fig. 2a represents the signal recorded at the far receiver location in the crosshole testing. The blue waveform was created by the coefficient of attenuation using Eqs. (2) and (3) with assumptions of: (1) the distance from source-to-near-receiver, r_1 = 3 m, (2) the distance from source-to-far-receiver, r_2 = 6 m, (3) shear wave velocity = 300 m/sec, and (4) damping ratio = 0.03 as shown in Fig. 2c.

To apply the half-power bandwidth method to crosshole signals, the shear wave velocity needs to be determined. The SABW method is applied to calculate the shear wave velocities at each frequency. As shown in Fig. 3a, the shear wave velocity is 300 m/sec over the frequency range of interest as designed. Once the shear

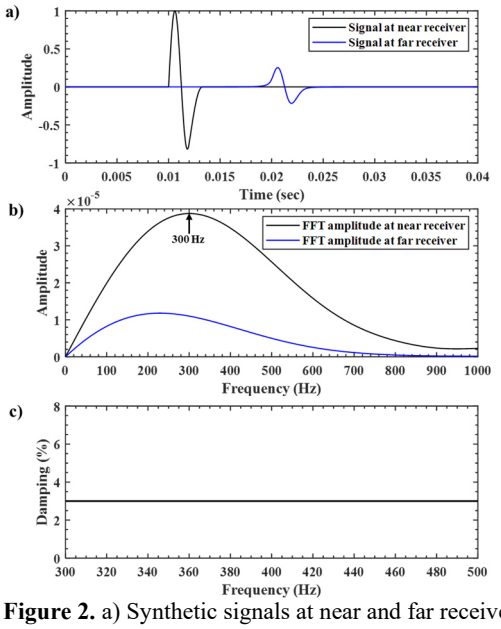

Figure 2. a) Synthetic signals at near and far receiver locations at the crosshole testing site (b) FFT amplitudes of the synthetic signals shown in Fig. 2a, and (c) material damping ratio calculated from synthetic signals shown in Fig. 2a

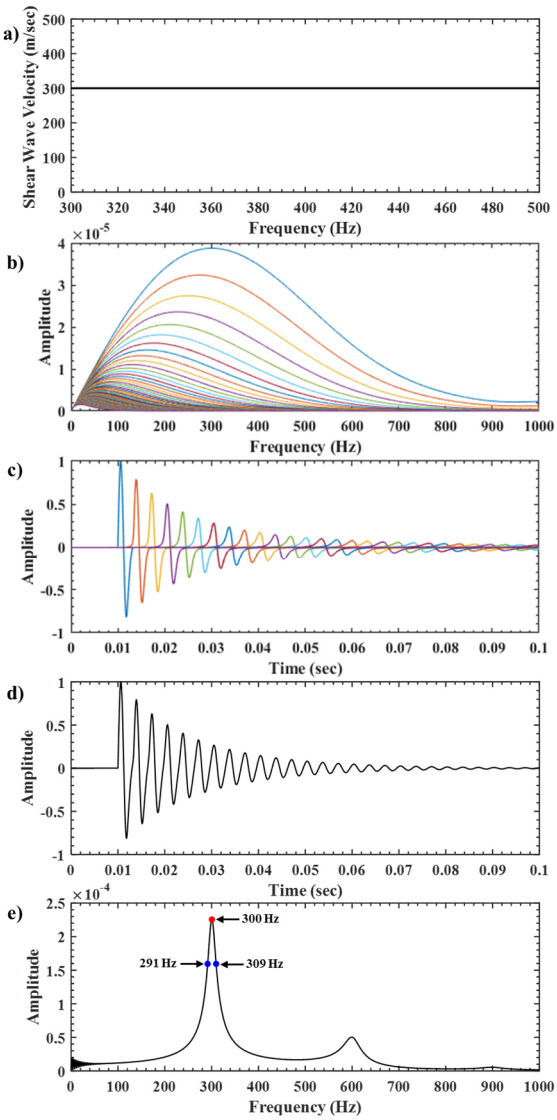

Figure 3. a) Shear wave velocity calculated using the near and far receiver synthetic signals, (b) amplitude of the FFT of the resonating signal, (c) resonating signal in the time domain, (d) sum of all signals in Fig. 3c, and (e) amplitude of the FFT of the added signal as shown in Fig. 3d.

wave velocity is calculated, the wave travel distance is simply determined by Eq. (12).

$$L = \frac{V}{f_{Amax}} \tag{12}$$

where V is the wave velocity of the structure, and f_{Amax} is the frequency of the maximum amplitude of the FFT determined from the near crosshole receiver signal. For the synthetic example, the wave travel distance is 1 m which is equal to the 50 cm sample in the Fr-Fr test. Then, the amplitude of the FFT from the near receiver signal is multiplied by β, the attenuation ratio, which is calculated using Eq. (11) with r_z from 4 m to the distance until the signal dissipates as shown in Figs. 3b and 3c. The amplitudes of the FFT of resonating signals are shown in Fig. 3b and the resonating signals are presented in the time-domain in Fig. 3c. Each color represents the signals recorded from the imaginary receivers located at every 1 m interval starting from 3 m. The signals are shifted based on the travel distance divided by the shear wave velocity as shown in Fig 3c. This sequence is the same as performing the Fr-Fr test of a 0.5-m long sample which has a shear wave velocity of 300 m/sec. Finally, all the signals in Fig. 3c are added as shown in Fig. 3d and the amplitude of the FFT of the added signal is presented in Fig. 3e. The material damping is calculated from Fig. 3e using Eq. (8) which results in a value of 0.03 as assumed. Since the frequencies are round values, there is a 0.17% error in this method. This error is negligible up to the material damping of 0.1 which is an assumption for the simplification of the half-power bandwidth method as discussed in Section 2. Even if the material damping is above 0.1, the error is still around 1~2%, and the small-strain material damping ratio for most geotechnical material is less than 0.1 (10%).

The synthetic signal used for the verification is close to the windowed signal. Because of this reason, the material damping ratio is the same between the half-power bandwidth and the coefficients of attenuation methods. For the analysis of complicated signals from in-situ testing data, the half-power bandwidth method will provide more reliable values as discussed in the next section.

5. Field tests

Two sets of crosshole and downhole tests were performed, one at the Hornsby Bend research site operated by the University of Texas at Austin and the second at a compacted backfill test pad. The half-power bandwidth method was applied to the in-situ crosshole test data and was verified by the Spectral Ratio Slope (SRS) method applied to the downhole test data performed at the same location. However, the SRS method only can be applied to the receiver locations deeper than 5 m, where the signal is not affected by surface layer interference.

The crosshole and downhole tests were performed from 0.9 to 11.9 m with a 0.9-m increment at the Hornsby Bend research site. The soil profile of this site is: 0 ~ 1.8 m of clay, 1.8 ~ 4.6 m of silty sand, 4.6 ~ 7.6 m of clay, 7.6 ~ 9.1 m of clay and silty sand mixture, and 9.1 ~ 11.9 m of silty sand layers. The SRS method was applied to the downhole signals recorded from 5.5 to 11.9 m, and Eqs. (4) and (5) were used to calculate the material damping ratio. The slopes of the spectral ratio from the depth of 5.5 to 11.9 m and the resulting values of the material damping ratio are shown in the lower part of Fig. 4. As seen in Fig. 4, the material damping ratio determined by the SRS method is an average of the clay and clay-silty sand mixture layers ranging from 6.4 to 9.1 m, resulting in a damping ratio of 6.72%. For the silty sand layer, the material damping ratio is 1.36%.

The material damping calculation by the half-power bandwidth method using the crosshole signal at the depth of 5.5 m is shown in Fig. 5 as an example of the field data analysis. The shear wave signals recorded at the near and far receivers are shown in Fig. 5a with black and blue lines, respectively. The first cycle of the shear wave signals are shown in green-dashed and red-dashed lines, respectively, in Fig. 5a to determine the influence of the windowed function. The half-power bandwidth method is applied to the full and windowed signals and the resulting values of material damping are compared as

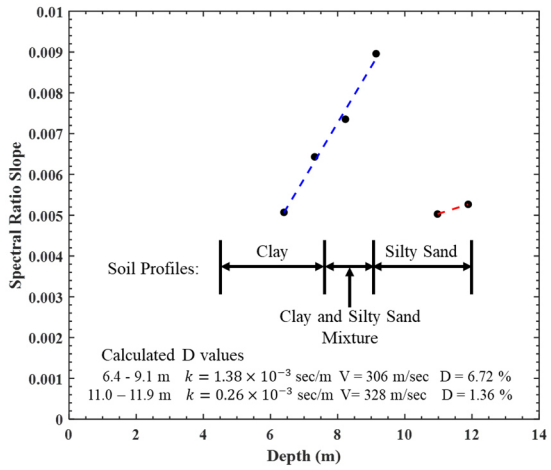

Figure 4. Material damping calculated by the SRS method applied to the downhole records at the Hornsby Bend Research Site

shown in tabular and graphical forms in Table 1 and Fig. 6. The amplitude of the FFT of the near and far receiver signals are shown in Fig. 5b. The frequency of the maximum amplitude of the FFT from the near receiver signal was 137 Hz, and it was used to calculate the wave travel distance by using Eq. (12).

As done with synthetic signals, the shear wave velocity is first calculated between the near and far receiver signals using the SABW method as shown in Fig. 5c. The frequency range of interest for the shear wave velocity is ± 5% of the maximum frequency as shown in Fig. 5c which results in 294 m/sec. The shear wave value is a major criterion deciding the integrity of the full signal. If the shear wave value of the full signal determined from the SABW method has more than a 10% difference with the shear wave velocity determined from the first cycle or from the picked first arrival point, the window function needs to be applied to separate the wave group. The wave segmentation can be done by using the watershed algorithm (Meyer 1994) and can be used as a guideline for assessing the integrity of the signal and the wave velocity calculation. The signals in Fig. 5a are determined as one wave group based on the wave segmentation guideline.

After the determination of the shear wave velocity, the attenuation ratio, β, is determined from Eq. (11), using the amplitude of the FFT at the near and far receiver signals. The wave travel distance is 2.15 m from Eq. (12). The resonating signals using the determined shear wave velocity, β, and travel distance from the crosshole signals at a depth of 5.5 m are presented in Fig. 5d and 5e in the frequency and time domain, respectively. The resonating signals in Fig. 5e are not dissipating since there is the frequency range where the amplitude is amplified as shown in Fig. 5d. This amplified range of the signal is theoretically impossible from wave propagation theory and sourcing from other than the crosshole trigger signal. However, if the amplification frequency is less than the half-power point as shown in Fig. 5g, there is no influence on the material damping calculation for the half-power bandwidth method. The β values for this range are set to 1. All signals in Fig. 5e are added as shown in Fig. 5f, and the amplitude of the FFT of the

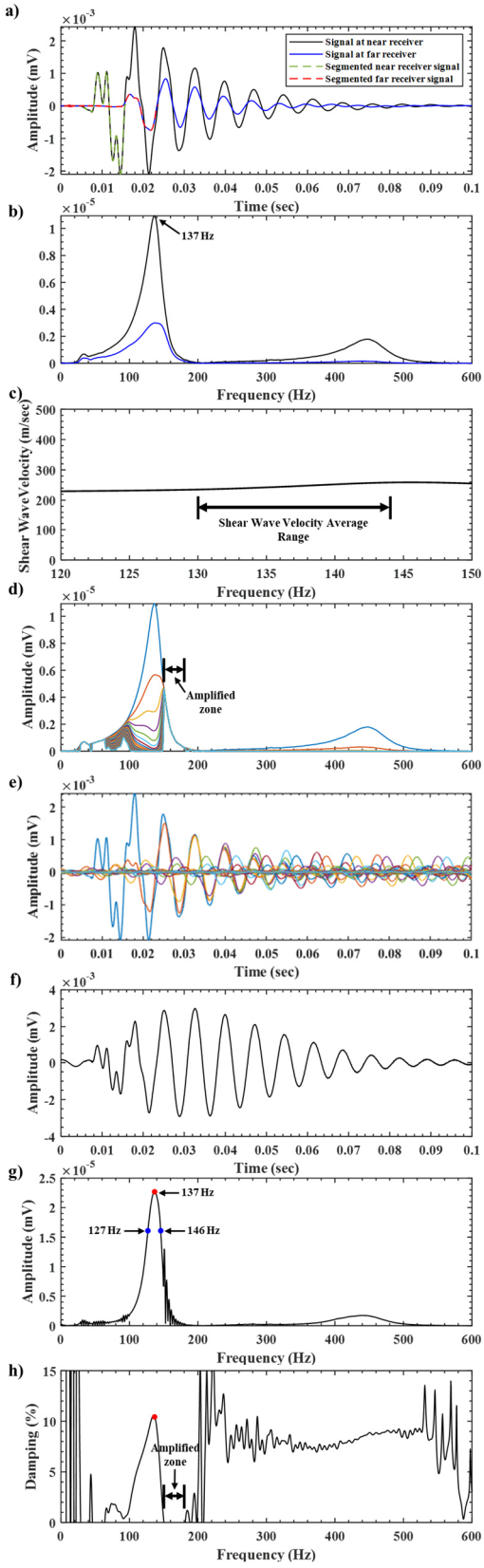

Figure 5. a) Crosshole signals from the near and far receiver locations at the Hornsby Bend Research Site (b) FFT amplitude of the crosshole signals shown in Fig. 5a, (c) shear wave velocity calculated using the near and far receiver signals, (d) amplitude of the FFT of the resonating signal, (e) resonating signal in the time domain, (f) sum of all signals in Fig. 5e, (g) amplitude of the FFT of the added signal as shown in Fig. 5f, and (h) material damping calculated using the coefficient of attenuation method

Table 1. Material damping ratio calculated using the half-power bandwidth and coefficient of attenuation methods for the first cycle of signal and full signal at the Hornsby Bend Research Site

	First cycle of signal		Full signal	
Depth (m)	Half-power Bandwidth (%)	Coeff. of Attenuation (%)	Half-power Bandwidth (%)	Coeff. of Attenuation (%)
0.9	5.07	5.08	7.47	12.44
1.8	10.26	10.18	10.66	12.03
2.7	6.7	6.69	5.07	6.15
3.7	4.15	4.18	6.30	9.14
4.6	2.68	2.69	3.54	4.96
5.5	2.92	2.92	6.93	10.43
6.4	5.27	5.18	6.91	24.29
7.3	6.47	6.52	6.10	25.56
8.2	3.66	3.67	4.37	11.22
9.1	3.03	3.00	2.69	4.21
10.1	2.22	2.20	1.17	1.17
11.0	1.82	1.76	1.58	2.50
11.9	3.51	3.53	1.79	4.43

added signal is presented in Fig. 5g. The material damping calculated from the half-power points as shown in Fig. 5g is 6.93%, which is close to the SRS material damping value of 6. 72% for the clay layer. The material damping calculated with the same signals using the coefficient of attenuation method is 10.43% higher than the SRS material damping value as shown in Fig. 5h in the red dot. The material damping for the amplified zone is negative for the coefficient of attenuation method.

The difference in material damping values for the complicated in-situ signals results from that while the coefficient of attenuation method uses only the shape of the amplitude of the FFT to calculate the material damping ratio, the half-power bandwidth method resonates the signal which can amplify or confine the amplitude of the frequency range of interest for the damping calculation. If the signals are windowed to create a simpler waveform like the first cycle of each signal, the material damping value will be the same for both methods as shown by comparing both columns under the First-cycle-of-signal heading.

The first cycle of the near and far receiver signals are also calculated using the half-power bandwidth method and the coefficient of attenuation methods. Both methods result in a value of 2.92% as shown in Table 1 which is one-third of the SRS material damping ratio. As shown in Table 1, the half-power bandwidth and coefficient of attenuation methods result in almost the same material damping values when the first cycle of the signal is used. Therefore, the material damping calculated from the first cycle of the signal using the coefficients of attenuation method is not shown in Fig. 6 for clarity. However, the average material damping for the clay layer from 5.5 to 7.3 m is 4.89% which is lower than the SRS value of 6.72%. The average material damping for the silty sand layer from 10.1 to 11.9 m is 2.52% which is almost two times higher than 1.36%. Therefore, the window function needs to be avoided in the material damping calculations.

When the full signal is used, the coefficient of attenuation method results in unreasonable material damping ratios between the depths of 5.5 to 8.2 m as indicated in Table 1 and Fig. 6. The average material damping value for the clay layer from the half-power

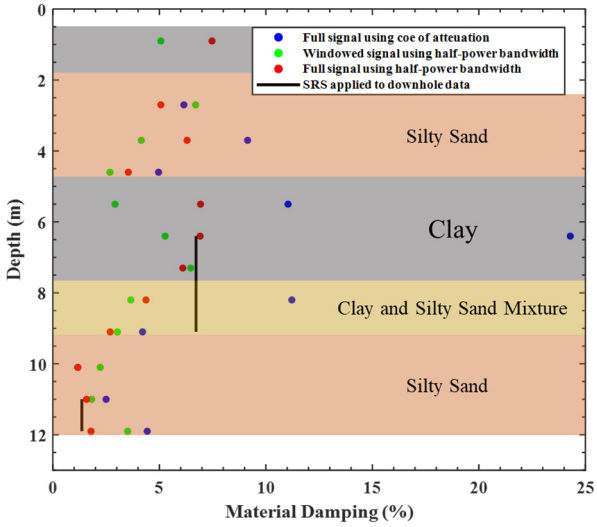

Figure 6. Comparison of material damping values determined by full signal using coefficient of the attenuation, windowed signal using half-power bandwidth, full signal using half-power bandwidth, and SRS applied to downhole data in the Hornsby Bend research site

bandwidth method using the full signal is 6.65% which is close to the SRS value of 6.72%. More importantly, the half-power method identifies the transition layer between the clay and silty sand layers as shown in Fig. 6.

The material damping values for the transition layer are 4.37 and 2.69%. The average material damping value for the silty sand layer from 10.1 to 11.9 m is 1.51% which is close to the SRS value of 1.36%. There are questions about the values in the silty sand layer from 2.7 to 4.6 m where the half-power bandwidth method results in an average value of 4.97%. However, for now, there is no other method to verify the in-situ damping of the shallow surface layer.

As part of a subsurface characterization program of a potential site for two nuclear power plants, a compacted backfill test pad was constructed. The objective of the test-pad construction was to assess the potential of on-site granular soils for fulfilling the requirements for a Category-1 compacted backfill as specified by the United States Nuclear Regulatory Commission. In total, 25 lifts of compacted backfill were placed, and the as-built total thickness equaled 6.2 m. Lifts 1 through 13 made up the lower approximately 3 m of the test pad which was mainly silty sand (SP-SM) with some clayey sand (SP-SC and SW-SC) layers. Somewhat coarser sand (SP) with less fines (2.4 %) was placed in Lifts 14 through 25 which made up the upper approximate 3.2 m of the test pad. The average Proctor compaction levels of the lower and upper portions of the granular backfill were 103 and 101 %, respectively (Stokoe et al, 2018).

The crosshole and downhole tests were performed from 1.2 to 7.9 m with a 0.6 m increment at the backfill test pad. The SRS method was applied to the downhole signals recorded from 4.9 to 6.7 m. The slope of the spectral ratio from 4.9 to 6.7 m and the resulting values of material damping are presented in Fig. 7. As seen in Fig. 7, the material damping of the SP-SM material is 2.72%.

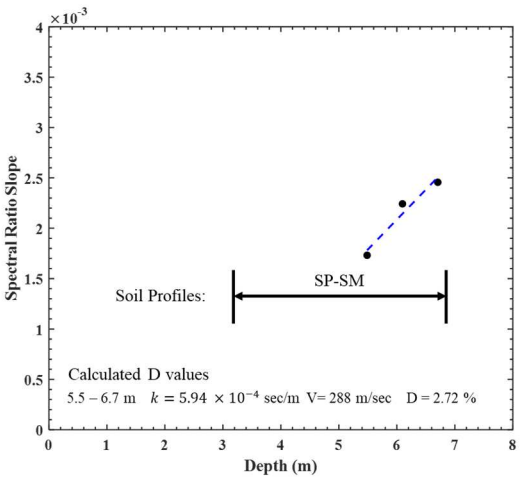

Figure 7. Material damping calculated by the SRS method applied to the downhole records at the backfill test pad

The summary of the material damping ratios calculated by the first cycle of the signal using the half-power bandwidth and the coefficient of attenuation, and by the full signal using half-power bandwidth and coefficient of attenuation methods are presented in tabular and graphical forms in Table 2 and Fig. 8. As shown in Table 2, the first cycle of the signal cannot be used for the material damping calculation at the few receiver depths since the amplitude at all frequencies range is amplified meaning negative material damping value at the frequency range of interest. The average material damping value calculated from the coefficient of attenuation method using the full signal for the SP-SM layer, except for the value at 3.7 m which has been influenced by the SP material, is 4.13%. This value is higher than the material damping calculated from the SRS value of 2.72 %. The average material damping value for the SP-SM layer from the half-power bandwidth method using the full signal is 2.53% which is close to the SRS value of 2.72%. More importantly, the half-power method identifies the material damping of the natural material which is 1.08%. In addition, the half-power method results in constant material damping of the SP material which averages about 1.67% as shown in Fig. 8.

Table 2. Material damping ratio calculated using the half-power bandwidth and coefficient of attenuation methods for the first cycle of the signal and full signal at the backfill test pad

	First cycle of signal		Full signal	
Depth (m)	Half-power Bandwidth (%)	Coeff. of Attenuation (%)	Half-power Bandwidth (%)	Coeff. of Attenuation (%)
1.2	2.72	2.72	1.61	1.71
1.8	0.63	0.45	1.64	2.6
2.4	-	-	1.56	1.72
3.0	-	-	1.87	3.02
3.7	-	-	1.12	1.2
4.3	1.68	1.69	2.93	3.46
4.9	1.15	1.12	2.29	3.35
5.5	-	-	2.27	3.76
6.1	1.84	1.84	2.63	5.94
6.7	1.52	1.49	1.22	0.83
7.3	-	-	1.12	1.62
7.9	-	-	0.89	1.12

- Negative material damping

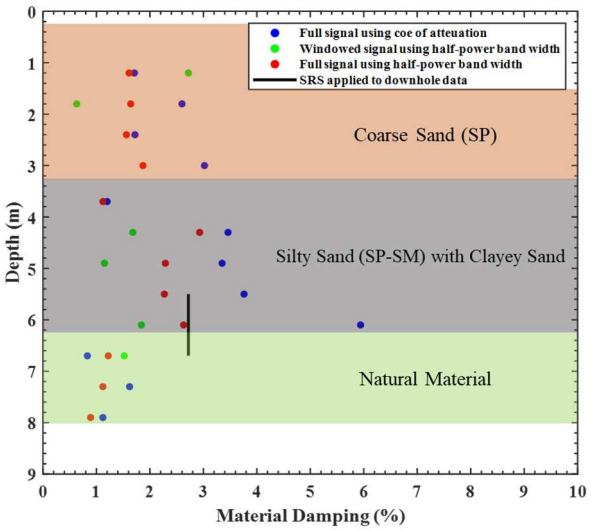

Figure 8. Comparison of material damping values determined by full signal using the coefficient of attenuation, windowed signal using half-power bandwidth, full signal using half-power bandwidth, and the SRS applied to downhole data at the backfill test pad.

6. Conclusions

In crosshole testing, the half-power bandwidth method is proposed for material damping calculations without the window function. The half-power bandwidth method amplifies or confines the amplitude of the frequency range of interest for the damping calculation which can be applied to complicated in-situ signals. The half-power bandwidth method is theoretically verified using synthetic signals and field data. The material damping calculated from the half-power bandwidth method using the full signal results in a reliable damping value compared to the SRS method applied to the downhole data. In addition, the half-power bandwidth method can only identify the material damping of transition layers. The influence of the window function is also studied by using the first cycle of the signal and the window function is recommended to avoid if possible.

References

Hwang, S. 2018. “Advanced data analysis techniques for downhole seismic testing.” Ph.D. Dissertation, The University of Texas at Austin, Austin

Karl, L., Haegeman, W., Degrande, G. 2006. “Determination of the material damping ratio and the shear wave velocity with the Seismic Cone Penetration Test.” Soil Dynamics and Earthquake Engineering, Volume 26, Issue 12, pp. 1111-1126. https://doi.org/10.1016/j.soildyn.2006.03.001

Meyer, F. 1994. “Topographic distance and watershed lines. Signal Processing.” Vol. 38, pp. 113-125.

Mok, Y.J, Sanches-Salinero, I, Stokoe, K.H. II., Roesset, J.M. 1988. “In Situ damping measurements by cross-hole seismic method.” Earthquake Engineering and Soil Dynamics II. ASCE Specialty Conference, Park City, U.S.A, pp. 305±20.

Richart, F.E. Jr., Hall, J.R. Jr., and Woods, R.D. 1970. “Vibrations of Soils and Foundations.” Prentice Hall Inc, New Jersey, U.S.A. pp. 414.

Stewart, W.P., and Campanella, R.G. 1991. “In situ measurement of damping of soils.” 2nd International Conference on Recent Advances in Geotechnical

Earthquake Engineering and Soil Dynamics, Rolla, U.S.A, pp. 83-92.

Stewart, W.P., and Campanella, R.G. 1993 “Practical aspects of in situ measurements of material damping with the seismic cone penetration test.” Canadian Geotechnical Journal. 30(2). https://doi.org/10.1139/t93-018

Stokoe, K.H. II., Hwang, S.K., Roesset, J.M., and Sun, W.S. 1994. “Laboratory measurements of small-strain material damping of soil using the free-free resonant column.” Earthquake Resistant construction and Design, Berlin, German, pp. 195-202.

Stokoe, K.H. II., Hwang, S., Boone, M., Lewis, M. R., Wang, Y., Cooke, M. F., and Keene, A. K. 2018. “Measured and Predicted Vs Values of a Granular Backfill Test Pad.” Conf on Geotechnical Earthquake Engineering and Soil Dynamics V, Austin, U.S.A, pp. 473-488.

Tonouchi, K., Sakayama, T., and Imai, T. 1983. “S wave velocity and the damping factor.” Bulletin of the International Association of Engineering Geology, 26/27, pp. 327-333.